

$\log I_a = -4.03$ ,  $\log I_c = -6.05$  (cf. Fig. 5), and  $R_t = 15 \text{ mV}/\mu\text{A}$ , resulting in  $\gamma_1 = 0.52$  and  $\gamma_2 = 0.007$ .

Although it is much more probable that  $\gamma \sim 0.5$  is the correct value the ambiguity arising from Eq. [17] having two roots can be removed by employing Eq. [16] with the values of the Tafel line intercepts and charge-transfer resistances obtained in two different sets of experiments. In this case

$$R_t = \frac{RT}{4F} \left( \frac{1}{I_a \gamma} + \frac{1}{I_c (1 - \gamma)} \right),$$

$$R_t' = \frac{RT}{4F} \left( \frac{1}{I_a' \gamma} + \frac{1}{I_c' (1 - \gamma)} \right) \quad [18]$$

$$\text{and} \quad \gamma = \frac{I_c - KI_c'}{K(I_a' - I_c') - (I_a - I_c)} \quad [19]$$

where  $K = R_t I_a I_c / R_t' I_a' I_c'$ .

Making use of the same experimental data as in the calculations above one finds  $\gamma = 0.5$ . Apart from the need of two separate sets of polarization data it is preferable to use Eq. [17] because the error in the calculation of  $\gamma$  using Eq. [19] can become quite appreciable due to the presence, in both numerator and denominator, of  $\Delta I$ 's. It should also be pointed out that the close agreement between the values of  $\gamma$  obtained with the two methods is, therefore, somewhat misleading and is attributable to the choice of suitable pairs of polarization curves. Equation [19] can, however, serve a useful purpose in deciding between the roots of Eq. [17]. The fact that  $\gamma$  is found to be so close to 0.5 demonstrates that on the time scale of the Gerischer extrapolation the current distribution of the steady state is rapidly reached and that the stationary concentration of  $S_m$  can differ only slightly from its thermodynamic equilibrium concentration.

Having thus ascertained the numerical value of  $\gamma$  it is now an easy matter to make a direct comparison between the exchange current densities of the toluquinhydrone and benzoquinhydrone electrodes. Taking Vetter's results and the data presented in this paper it is seen that, at corresponding concentrations, the

exchange current densities of the toluquinhydrone electrode are invariably higher, at some concentrations by as much as a factor of about 300. It seems therefore that the toluquinhydrone electrode should function as the superior indicator and reference electrodes from the point of view of its greater reversibility. This advantage will, however, in most practical cases be negated by the easy photodecomposition of its electrolyte solution.

#### Acknowledgments

The author wishes to express his gratitude to C. F. Cook for his help in setting up the triggering circuit for the oscilloscopic measurements, and to W. F. Nye for his continued interest and encouragement.

Manuscript received May 9, 1972. This was Paper 248 presented at the New York Meeting of the Society, May 7-9, 1969.

Any discussion of this paper will appear in a Discussion Section to be published in the June 1973 JOURNAL.

#### REFERENCES

1. K. J. Vetter, *Z. Elektrochem.*, **56**, 797 (1952).
2. J. H. Hale and R. Parsons, *Trans. Faraday Soc.*, **59**, 1429 (1963).
3. B. R. Eggins and J. Q. Chambers, *This Journal*, **117**, 186 (1970).
4. M. Loshkarev and B. I. Tomilov, *Zhur. Fiz. Khim.*, **34**, 1753 (1960).
5. M. Loshkarev and B. I. Tomilov, *ibid.*, **36**, 132 (1962).
6. M. Loshkarev and B. I. Tomilov, *ibid.*, **36**, 1902 (1962).
7. E. A. Cooper and S. D. Nicholas, *J. Soc. Chem. Ind. (London)*, **46**, 59T (1927).
8. D. J. G. Ives and G. J. Janz, "Reference Electrodes," p. 209, Academic Press (1961).
9. H. Gerischer, *Z. Elektrochem.*, **59**, 604 (1955).
10. K. J. Vetter, *Z. Naturforsch.*, **7a**, 328 (1952).
11. K. J. Vetter, *ibid.*, **8a**, 823 (1953).
12. R. M. Hurd, *This Journal*, **109**, 327 (1962).
13. H. Gerischer and K. J. Vetter, *Z. Phys. Chem.*, **197**, 92 (1951).
14. e. g., K. J. Vetter, *ibid.*, **194**, 284 (1950).
15. C. Wagner and K. Gruenwald, *Z. Elektrochem.*, **46**, 265 (1940).

## The Electrochemistry of the Liquid Crystal N-(p-Methoxybenzylidene)-p-n-butylaniline (MBBA) The Role of Electrode Reactions in Dynamic Scattering

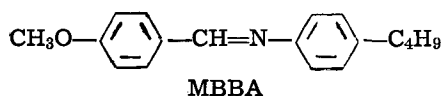
Ann Lomax, Ryo Hirasawa, and Allen J. Bard\*

Department of Chemistry, The University of Texas at Austin, Austin, Texas 78712

#### ABSTRACT

The electrochemical reduction and oxidation of MBBA were studied by cyclic voltammetry and by controlled potential coulometry. The reduction in DMF leads to the formation of the radical anion which decomposes with a half-life of about 4 sec, apparently by both ec and ece pathways. The oxidation product was unstable on the time scale of this study. The possible importance of electrode reactions in interpreting the dynamic scattering phenomenon in nematic liquid crystals is suggested.

The liquid crystal (LC) Schiff base N-(p-methoxybenzylidene)-p-n-butylaniline (MBBA) has been of much recent interest because it undergoes "dynamic

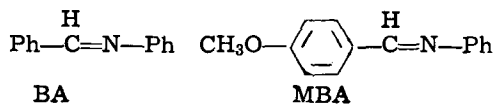


\* Electrochemical Society Active Member.  
Key words: electro-organic chemistry, cyclic voltammetry, coulometry, electron spin resonance, Schiff base.

scattering" (DS) when subjected to d-c or a-c electrical fields; this electrooptic effect forms the basis of LC display devices. Dynamic scattering has been shown to occur when the LC, sandwiched between two closely spaced (e.g., 10-100  $\mu\text{m}$ ) electrodes above a certain threshold voltage, begins to undergo first laminar and then turbulent flow (1). The mechanism of this phenomenon has been the subject of a number of recent studies (2-8) and is apparently different for d-c and low frequency a-c excitations, where the electrodes

must contact the LC phase, and for high frequency a-c excitations, where the electrodes may be insulated or "blocked" from the LC. The d-c low frequency mechanism is based on the "injection of electrons" into the low conductivity LC leading to space charges; transfer of momentum from the resulting moving ions under the influence of the field to the aligned LC molecules results in cellular hydrodynamic flow (1-3). In an alternate model the space charges in the nematic LC originate in the anisotropic conductivity of the LC (4-6). These models generally ignore the electrochemical processes occurring at the electrode-LC interface and the nature of the ionic species formed in the process. Because these processes can affect the threshold voltage for the onset of dynamic scattering and have important ramifications in the occurrence of secondary chemical reactions which may limit the life of the LC device, we have undertaken a study of the electrochemical behavior of LC materials.

Most of the electrochemical studies of MBBA described here were performed using the aprotic solvents *N,N*-dimethylformamide (DMF) or acetonitrile (ACN) as reaction media; a few preliminary studies in neat MBBA were also attempted, however. Previous electrochemical studies on the reduction of the related molecule, *N*-benzylideneaniline (BA) (9-12) and the oxidation of *N*-(*p*-methoxybenzylidene)aniline (MBA) (13) have been described.



### Experimental

The MBBA was special, high-purity material obtained from Texas Instruments. The supporting electrolyte materials, tetra-*n*-butylammonium perchlorate (TBAP) and iodide (TBAI), were polarographic grade (Southwestern Analytical Chemicals) and were dried in a vacuum oven before use. Purification of the solvents DMF and ACN followed previous practice (14, 15).

All electrochemical data were obtained with a Princeton Applied Research Corporation (PAR) Model 170 electrochemical system. Solution preparation on a vacuum line and freeze-pump-thaw techniques were as previously described (14, 15). The cell for voltammetric studies contained either a platinum disk or a hanging mercury drop working electrode, a platinum auxiliary electrode in a separate chamber, and an aqueous saturated calomel electrode (SCE) connected to the test solution by an agar bridge with its tip positioned near the working electrode. The coulometric studies were done in the same cell with a platinum gauze working electrode. Electron spin resonance (ESR) spectra were obtained on a Varian V-4502 spectrometer and electrolytic cell accessory. The solutions were degassed by the freeze-pump-thaw method and transferred to a reservoir above the ESR electrolytic cell. The cell was flushed with nitrogen and fresh solution from the reservoir was employed for each experiment.

### Results

**Electrochemical reduction.**—The reduction of MBBA at a platinum electrode was studied by both cyclic voltammetry and controlled potential coulometry to obtain information about the electrochemical behavior of the system on both a short and a long time scale. A typical cyclic voltammogram for the reduction in DMF is shown in Fig. 1. The first reduction wave occurs at  $-2.06\text{V vs. SCE}$  and is nearly reversible at scan rates above 5 V/sec. The second reduction wave occurs at  $-2.60\text{V}$  and shows no reversal current even at high scan rate. The reduction potential of the first wave is more negative than that of BA ( $-1.83\text{V}$ ) (9) as expected for the introduction of an electron-donating group into the molecule, and is close to that for MBA ( $-2.15\text{V}$ ) (10) in DMF solutions.

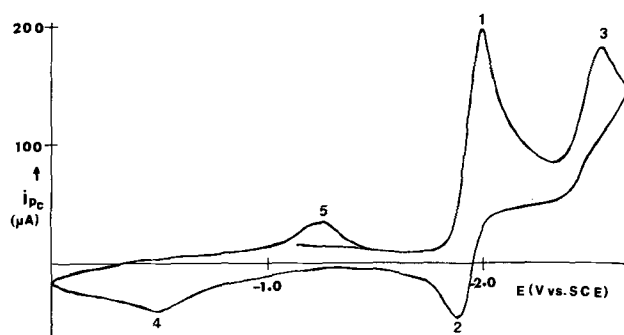


Fig. 1. Cyclic voltammogram at a Pt disk electrode of 6.65 mM MBBA in DMF, 0.1M TBAP. The scan rate was 2 V/sec.

Figure 1 shows, in addition to the two major reduction waves of MBBA (1, 3) and the oxidation of MBBA<sup>-</sup> (2), two waves of lesser height. An anodic wave (at  $-0.54\text{V}$ ) (4) appears to a slight extent after scanning through only the first wave, and to a greater degree if the scan is continued beyond the second main reduction wave. The small cathodic wave (at  $-1.38\text{V}$ ) (5) appears only after having scanned through wave 4. Neither the nature nor the source of these waves was investigated. The anodic wave 4 was found to be the only wave remaining after exhaustive electrolysis of the solution at a potential on the plateau of the first wave. The behavior of the diagnostic criteria,  $i_{pa}/i_{pc}$  and  $i_{pc}/v^{1/2}$ , for the first reduction wave is shown as a function of scan rate,  $v$ , in Fig. 2 ( $i_{pc}$  and  $i_{pa}$  are the cathodic and anodic (reversal) peak currents, respectively). The peak height and peak potential separation, as well as the coulometric and ESR results below, show that the first reduction wave leads to the production of the radical anion in a one-electron reaction. The upper curve (Fig. 2a) illustrates the extent of reaction of the radical anion; the reaction is nearly complete at slow scan rates, while at fast scan rates it has scarcely begun. The qualitative shape of curve 2a is characteristic of both the ec and ece mechanisms, where an ec mech-

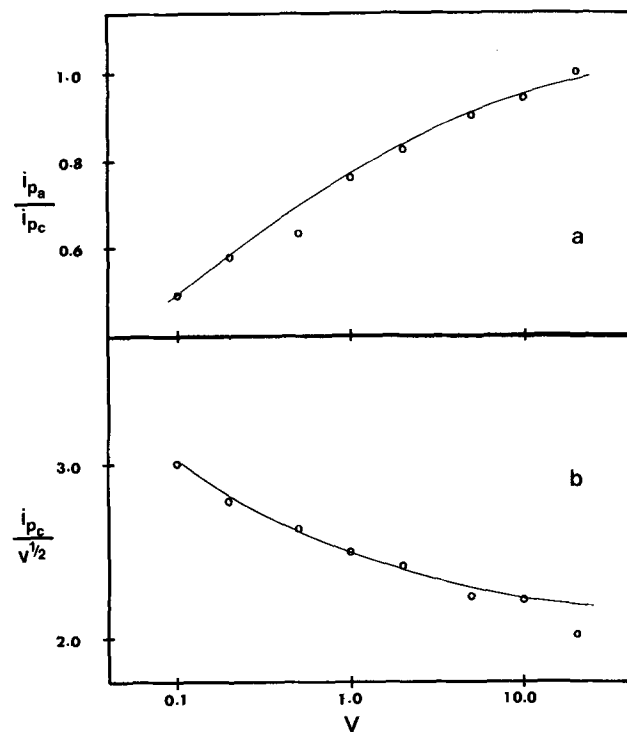


Fig. 2. (a) The peak current ratio, and (b) the normalized cathodic peak current vs. scan rate for the reduction at a hanging mercury drop electrode of 1.66 mM MBBA in DMF, 0.01M TBAP.  $v$  is in V/sec,  $i_{pc}/v^{1/2}$  in  $\mu\text{A sec}^{1/2}/\text{V}^{1/2}$ .

anism involves reaction of the electrogenerated product to a nonelectroactive species, while an ece mechanism implies that the product of the chemical reaction is reduced at potentials where MBBA is reduced. The data in Fig. 2b are useful in distinguishing between the two. In the ec case, the maximum change is about 10% while for the ece case, in which the product of the reaction is more easily reduced than the starting material, a maximum change of 50% can be observed (16, 17). The change of about 33% observed in the reduction of MBBA indicates a significant degree of ece behavior. The effect of  $v$  on the peak potential (Table I) is to shift the peak to more negative values at faster scan rates, as would be expected for an irreversible chemical reaction following electron transfer.

Exhaustive controlled potential coulometric reduction on the plateau of the first reduction wave gave an apparent number of faradays per mole of MBBA,  $n_{app}$ , of 1.2 to 1.9.

In ACN only the first reduction wave of MBBA was observed. Its peak potential was more negative ( $-2.15V$ ) than in DMF ( $-2.06V$ ); no reversal current was detected, even at scan rates of 20 V/sec.

**Electrochemical oxidation.**—The oxidation of MBBA in ACN occurs in two steps; a typical cyclic voltammogram is shown in Fig. 3. Waves 1 (1.45V) and 2 (2.0V) correspond to the oxidation of MBBA, while wave 3 is present in the solvent-supporting electrolyte medium before the addition of the depolarizer. Similar two-step oxidations have been reported for other Schiff bases (13). A small wave at 0.8V is also evident and is presumably caused by an impurity in the MBBA.

Though the occurrence of the second wave at a potential where the residual current is large makes its analysis difficult, a study of the peak characteristics of the first wave indicated that both the peak potential and the normalized peak current were dependent on the scan rate; the behavior is shown in Fig. 4, with the poor reproducibility of the current and potential measurements probably resulting from electrode filming. Neither wave yielded a detectable reversal current at scan rates up to 20 V/sec.

An  $n_{app}$  value determined by controlled potential coulometry at the first wave ranged from 0.88 to 1.2 electrons/molecule; the major electroactive product of the oxidation was reducible at  $-0.8V$ .

Attempts to investigate the electrochemical behavior of neat MBBA using TBAP or octadecyldimethylbenzylammonium bromide as supporting electrolytes in a small three-electrode cell were thwarted by the low solubility of the salts in MBBA and the concomitant low conductivity. The solution of MBBA with 15 volume per cent (v/o) DMF and TBAP had background limits of  $-1.8V$  corresponding to the reduction of MBBA, and  $+0.8V$ , probably the oxidation of the impurity noted in the oxidation of MBBA; there was no significant electrochemical process detected between the two limits.

**Electron spin resonance results.**—*Intra muros* electrolysis of a 1.5 mM MBBA solution in 0.1M TBAP-DMF at a constant current of 0.2 mA resulted in the ESR spectrum shown in Fig. 5. Attempts to simulate the spectrum and extract coupling constants have thus far been unsuccessful. Alkali metal reduction in MTHF did not produce a radical sufficiently stable to be detected.

Table I. Peak potentials for reduction waves of MBBA<sup>(a)</sup>

$v$ , V/sec	V vs. SCE $-E_{pc}$ (1)	V vs. SCE $-E_{pc}$ (2)
0.2	2.04	2.54
2.0	2.06	2.60
20.0	2.08	2.66

<sup>(a)</sup> The solution was 0.1M TBAP in DMF, 6.65 mM MBBA; the electrode, a Pt disk.

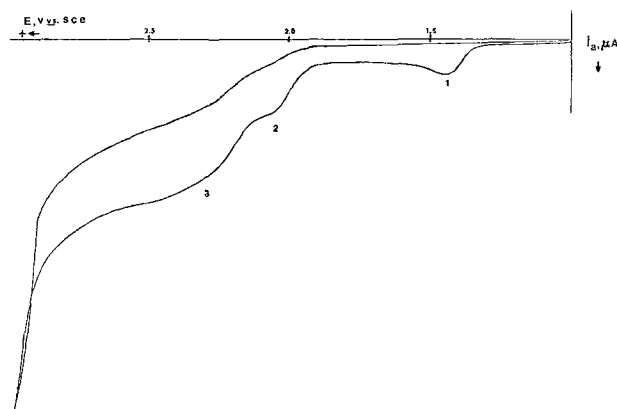


Fig. 3. Cyclic voltammogram at a Pt disk electrode of 2.24 mM MBBA in ACN, 0.1M TBAP. The scan rate was 0.2 V/sec.

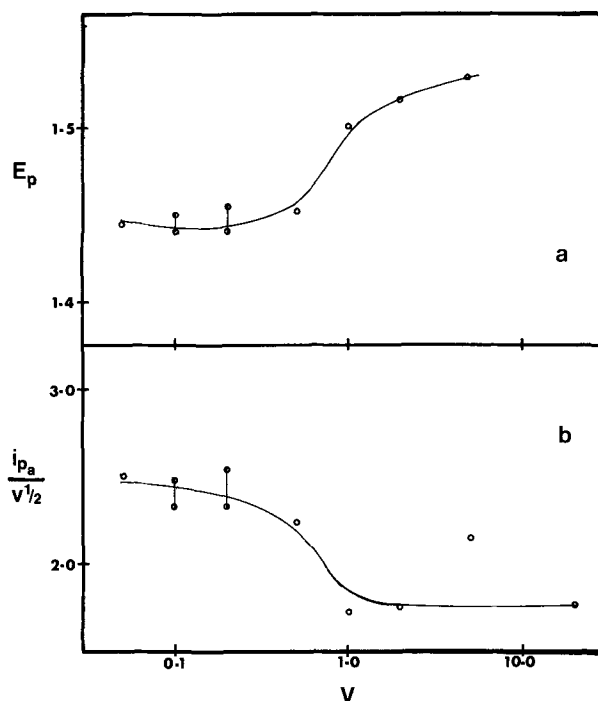


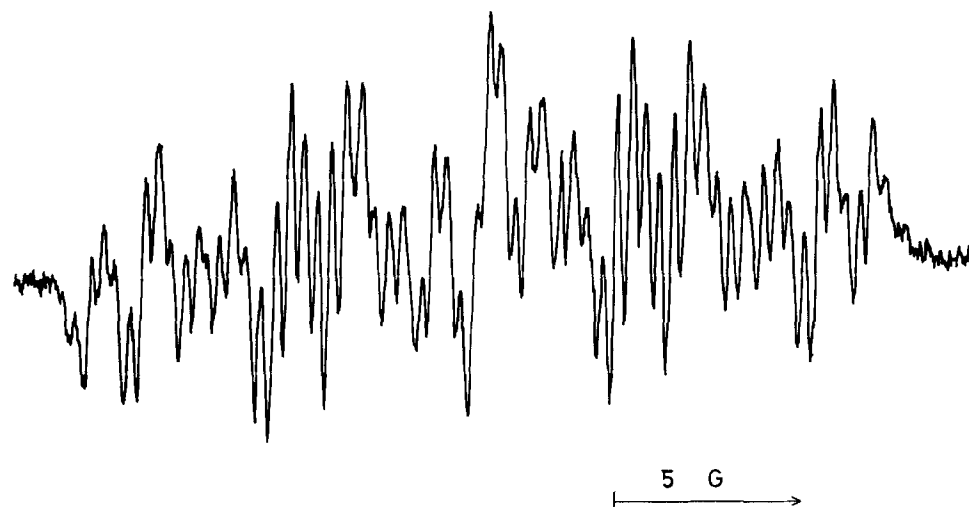
Fig. 4. (a) The peak potential, and (b) the normalized anodic peak current vs. scan rate for the oxidation at a Pt disk electrode of 2.24 mM MBBA in ACN, 0.1M TBAP.  $v$  is in V/sec,  $E_p$  in V vs. sce;  $i_{pa}/v^{1/2}$  in  $\mu A \text{ sec}^{1/2}/V^{1/2}$ .

A few experiments were performed in the SEESR cell (18) to determine the stability of the radical anion and the potentials where it is formed. For a constant-current pulse where the potential remained on the first voltammetric wave, the ESR signal showed a linear increase during the pulse, and a slow decay when the current was off. Constant-current steps where the potential reached those of the second wave showed a decrease of ESR signal at these potentials.

## Discussion

The electrochemical and ESR results for the reduction provide evidence for initial formation of the anion radical of MBBA with a half-life in DMF of approximately 4 sec. The evidence suggests that the radical anion reacts in following ece and ec reactions. Similar behavior has been reported for the reduction of BA (9-12), where both protonation (in the ece pathway) leading to conversion of the  $-HC=N-$  structure to  $-CH_2-NH-$ , and dimerization (in the ec pathway) occur. Andrieux and Saveant (9) and Kononenko *et al.* (11) concluded that both pathways were important and occurred simultaneously. Note that by labeling the protonation reaction as ece we only imply a reac-

Fig. 5. The ESR spectrum of the MBBA radical anion in DMF, 0.1M TBAI.



tion pathway leading to ultimate consumption of two electrons per molecule and do not reject other possible paths (e.g., disproportionation followed by protonation of the dianion) which may yield similar voltammetric and coulometric behavior.

The oxidation of MBBA in ACN parallels a previous study (13) and suggests that the oxidation product (perhaps the cation radical) is very unstable within the voltammetric time scale of these experiments.

Although these experiments were conducted in dilute solutions of MBBA in DMF and ACN rather than in pure MBBA, the results should have some relevance to dynamic scattering studies in MBBA. The measured potentials for reduction and oxidation here are probably somewhat smaller than those for the same processes in MBBA, since the polar solvents DMF and ACN probably solvate the MBBA ions more strongly than MBBA itself. Moreover, the fast reaction following the oxidation electron transfer reaction in ACN shifts the  $E_{pa}$  to values less positive than its reversible value. As a first approximation, however, we can take the "decomposition voltage" of MBBA as at least  $E_{pa}(\text{ACN}) - E_{pc}(\text{DMF})$ , or about 3.5V. The threshold voltage of dynamic scattering must be above this value and include the IR-drop through the MBBA liquid layer at currents (or ion flows) sufficient to induce turbulence. Although previous explanations of DS were given in terms of charge injection and Schottky emission of carriers (1), the current-voltage behavior was independent of the work functions of the metal used for the electrodes. Descriptions in terms of electrogeneration of radical ions and a cell current-voltage characteristic determined by the electrode kinetic equations (which bear a close resemblance to the Schottky emission equation) (19) and resistive drop in the liquid bear consideration. In a recent investigation (20), it was found that trace amounts of water are necessary in an anisylidene-p-aminophenylacetate (APAPA) LC device to promote conduction and DS; this was explained by a model in which water molecules assist the APAPA molecule in accepting an electron from the cathode. A more probable explanation in terms of our study is that ions from water (or hydrolysis products of APAPA) increase the conductivity of the LC material and improve the nature of the electrochemical cell. Doping of the LC with small amounts of different salts should serve the same purpose and decrease the possibility of attack of water molecules on the radical ions. Decomposition of the radical ions, particularly the radical cation, into products which decrease the purity and disrupt the alignment of the molecules in the nematic LC may also be of importance in limiting the life of LC display devices. Finally, although migration of the ions is probably the major mode of conduction through the liquid medium, direct electronic conduction by means of rapid electron exchange between radical ion and parent molecule is also a possibility,

especially in a solvent composed of pure parent molecules where the parent concentration is very high (21, 22). This conduction mode may be of less importance in this LC system, however, where the alignment of the molecules and structural considerations (i.e., the presence of the nonconjugated n-butyl group) decrease the rate of the intermolecular electron transfer reaction.

#### Acknowledgments

The support of this research by the National Science Foundation (GP-31414X) and the Robert A. Welch Foundation is gratefully acknowledged. We are indebted to Drs. Isaac Trachtenberg, Linda Creagh, and Allen R. Kmetz of Texas Instruments for helpful discussions concerning this research and for pure samples of MBBA.

Manuscript submitted June 12, 1972.

Any discussion of this paper will appear in a Discussion Section to be published in the June 1973 JOURNAL.

#### REFERENCES

- G. H. Heilmeyer, L. A. Zanoni, and L. A. Barton, *Proc. IEEE*, **56**, 1162 (1968).
- B. J. Lechner, F. J. Marlowe, E. O. Nester, and J. Tufts, *ibid.*, **59**, 1566 (1971).
- N. Felici, *Rev. Gen. Elec.*, **78**, 717 (1969).
- W. Helfrich, *J. Chem. Phys.*, **51**, 4092 (1969).
- P. A. Penz, *Mol. Cryst.*, **15**, 141 (1971).
- E. W. Aslaksen, *ibid.*, **15**, 121 (1971).
- H. Gruler and G. Meier, *ibid.*, **12**, 289 (1971).
- W. H. deJen and C. J. Gerritsma, *J. Chem. Phys.*, **56**, 4752 (1972).
- C. P. Andrieux and J. M. Saveant, *J. Electroanal. Chem.*, **33**, 453 (1971).
- P. Martinet, J. Simonet, and J. Tendil, *Compt. Rend. Acad. Sci. Paris*, **268**, 303 (1969).
- L. V. Kononenko, V. D. Bezuglyi, and V. N. Dmitrieva, *J. Gen. Chem. USSR*, **38**, 2087 (1968).
- J. M. W. Scott and W. H. Jura, *Can. J. Chem.*, **45**, 2375 (1967).
- P. Martinet, J. Simonet, and J. Tendil, *Compt. Rend. Acad. Sci. Paris*, **268**, 2329 (1969).
- L. R. Faulkner and A. J. Bard, *J. Am. Chem. Soc.*, **90**, 6284 (1968).
- L. S. Marcoux, A. Lomax, and A. J. Bard, *ibid.*, **92**, 243 (1970).
- R. S. Nicholson and I. Shain, *Anal. Chem.*, **36**, 706 (1964); *ibid.*, **37**, 178 (1965).
- M. Mastragostino, L. Nadjo, and J. M. Saveant, *Electrochim. Acta*, **13**, 721 (1968).
- I. B. Goldberg and A. J. Bard, *J. Phys. Chem.*, **75**, 3281 (1971).
- J. O'M. Bockris and A. K. N. Reddy, "Modern Electrochemistry," pp. 32, 942, Plenum Press, New York (1970).
- G. H. Heilmeyer, L. A. Zanoni, and L. A. Barton, *IEEE Trans. Electron Devices*, **ED-17**, 22 (1970).
- I. Ruff, *Electrochim. Acta*, **15**, 1059 (1970).
- H. Dahms, *J. Phys. Chem.*, **72**, 362 (1968).